ЖУРНАЛ СТРУКТУРНОЙ ХИМИИ

2013. Том 54, № 4 *Июль – август* *С. 631 – 638*

UDC 541.6:548.737

STRUCTURE AND INTERACTION BETWEEN THE [BMIM][Ala] ALANINE ANION AND THE 1-BUTYL-3-METHYLIMIDAZOLIUM CATION IN ION PAIRS

Z.W. Li[1], W.S. Wu[1], Z.Y. Du[2], X.Y. Hao[1]

[1]*College of Chemistry and Chemical Engineering, Zhaoqing University, Zhaoqing 526061, China*
E-mail:lzwgzzd@163.com
[2]*School of Light Industry and Chemical Engineering, Technical University of Guangdong, Guangzhou 510006, P. R. China*

Received March, 12, 2012

The equilibrium geometries and vibrational frequencies of the ionic liquid 1-butyl-3-methylimidazolium cation and the alanine anion [BMIM][Ala] are studied using density functional theory (DFT) at the B3PW91/6-311+G(*d*,*p*) leve1. The most stable structures of the anion, the cation, and the ion pairs are obtained and characterized, and the geometry parameters of the ion pairs confirm the presence of a hydrogen bonding interaction between the anion and the cation. Natural bond orbital (NBO) analysis is also performed to analyze the atomic charge distribution and charge transfer in the $[BMIM]^+$ cation and [BMIM][Ala] ionic liquids. The results show that there are the electrostatic interaction and multiple hydrogen bond interactions between the cation and the anion of the ionic liquids, and the stability of the ground state of the ion pairs mostly results from the hydrogen bonding between the lone pairs of O atoms in the anion and H in the imidazole cycle of the cation. There are some changes in microstructures and the charge distribution during the formation of the ion pairs.

K e y w o r d s: amino acid ionic liquids (AAILs), density functional theory (DFT), natural bond orbital (NBO), second order interaction energy.

INTRODUCTION

In recent years, ionic liquids (ILs) have been used widely in various chemical fields such as catalysis, organic synthesis, electrochemistry, biochemistry, and material engineering [1—4] due to their unique properties, including negligibly small vapor pressure, high thermal stability, and high ionic conductivity [5—7]. In addition, as an environmentally friendly solvent, ILs were expected to substitute the traditional industrial organic solvents, most of which resulted in environmental pollution because of their properties of volatility and toxicity. The coupling of the imidazolium cation with natural amino acids or the coupling of the amino acid cation with other anions can develop a novel concept of amino acid ionic liquids (AAILs) composed of natural amino acid ions. These AAILs not only possess the particular physical and chemical properties mentioned above, but also possess some great merits, such as low costs, are biodegradable and biocompatible, containing multi-functional groups, a strong hydrogen bonding ability and abundant source [8, 9], as revealed by the works of the groups of Ohno [9, 10] and Kou [11, 12]. In addition, the physicochemical properties of AAILs can easily be adjusted by modifying their various functional groups on the side chain of the amino acids [13, 14], therefore, the functional design of AAILs can be achieved for a wide range of tasks, for example, by introducing the chiral center into the IL [11—18].

Applications in the synthesis of AAILs as catalysts were published one after another, indicating that it is a pop field [19]. However, the mechanism of the reaction was a pending problem, and there-

fore the understanding of the properties of AAILs and the interpretation of the mechanism of catalysis were of fundamental importance not only for synthetic chemistry, but also for designing task-specific ILs. Therefore, apart from these experimental results, many theoretical papers were published [20—28] on the studies of their microstructures, intermolecular interactions, hydrogen bonds, and physicochemical properties. They included traditional molecular dynamics simulations, first-principles molecular dynamics simulations, and electronic structure methods. For example, AAIL of [emim][Gly] formed by the glycine anion demonstrated that the intermolecular H bonds were the evident characterristics of it [20]. By means of a combination of the experimental and theoretical methods, Rong *et al*. [21] studied the glutamic acid based ILs of [Glu]X(X = BF_4^-, NO_3^-, Cl^-, PF_6^-, …) and found that the smaller the absolute value of the binding energy between $[Glu]^+$ and the acid anion, the lower the melting point was. Gao *et al.* [22] carried out a theoretical study on the structure and the cation-anion interaction of $[Pro]^+[NO_3]^-$ AAIL, and Chiappe [23] studied the novel glycerol borate-based ILs by combining the experimental and theoretical studies. Zhang *et al.* [24] characterized the structural properties of *N*,*N*-dimethylformamide based IL using a DFT calculation. Gutowski *et al.* carried out the *ab initio* calculations on the formation and stabilities of ILs [25, 26]. Zhang *et al.* completed the DFT study on the structure and the cation-anion interaction of $[C_3mim]^+[Glu]^-$ AAIL [27]. Wu *et al.* explored systematically the structural and electronic properties of AAILs using a theoretical method and found that the properties of AAILs were dependent on the variety of amino acid anions [28]. These theoretical studies mentioned above redound to understand the molecular level interaction and further to predict and design functional AAILs.

In this paper, the structural and electronic properties of AAIL of the 1-butyl-3-methylimidazolium cation and the alanine anion, i.e. [BMIM][Ala], which was utilized as halogen-free catalyst for the synthesis of cyclic carbonates from CO_2 and epoxides [19], were explored by DFT. The results were useful for the understanding of the structures and properties of AAILs in the liquid phase and the interpretation of the mechanism of the catalysis, and furthermore, they contribute to the design of task specific ILs.

COMPUTATIONAL METHOD

The equilibrium geometries, vibrational frequencies, and interaction energies of [BMIM][Ala] were studied by performing DFT calculations. The B3PW91 [29, 30] method with the 6-311G+(*d*,*p*) basis set was used because B3PW91 would give a more reasonable description than other functionals [31], such as B3LYP, for AAIL involving strong hydrogen bonds. The electronic properties, bonding characteristics, and second order stability energies were illustrated based on the natural bond orbital (NBO) analysis [32, 33].

The interaction energy (ΔE_{int}) could be used to estimate the intensity of the interaction between the cation and the anion in ion pairs, which was defined as a difference between the energy of the ion pairs and the energies of their free fragments, and it can be evaluated in Eq.(1): $\Delta E_{int} = E_{cation} + E_{anion} - - E_{ionpair}$ where $E_{ionpair}$ is the energy of the ion pairs of [BMIM][Ala], E_{cation} is the energy of $[BMIM]^+$, and E_{anion} is the energy of $[Ala]^-$. In addition, the interaction energies were corrected by the basis set superposition errors (BSSE) [34] with the counterpoise procedure method [35] and the zero-point energy (ZPE) obtained within the harmonic approximation. All calculations were performed using the Gaussian-03 program [36].

RESULTS AND DISCUSSION

Geometries of [BMIM][Ala]. Initially, a series of possible geometries for the ion pairs were designed and optimized. However, some different initial geometries were optimized to the same result. After the optimizing process, seven various configurations named as **A**, **B**, **C**, **D**, **E**, **F**, and **G** of [BMIM][Ala] were obtained and illustrated in Fig. 1. The relative energies (E_r) corrected by ZPE, the interaction energies between the anion and the cation corrected by BSSE and ZPE ($\Delta E_{BSSE+ZPE}$), and the single point energy change or deformation energies (ΔE_{sp}) of the anion and the cation during the formation of [BMIM][Ala] are given in Table 1. At this level, the most stable isomer of [BMIM][Ala]

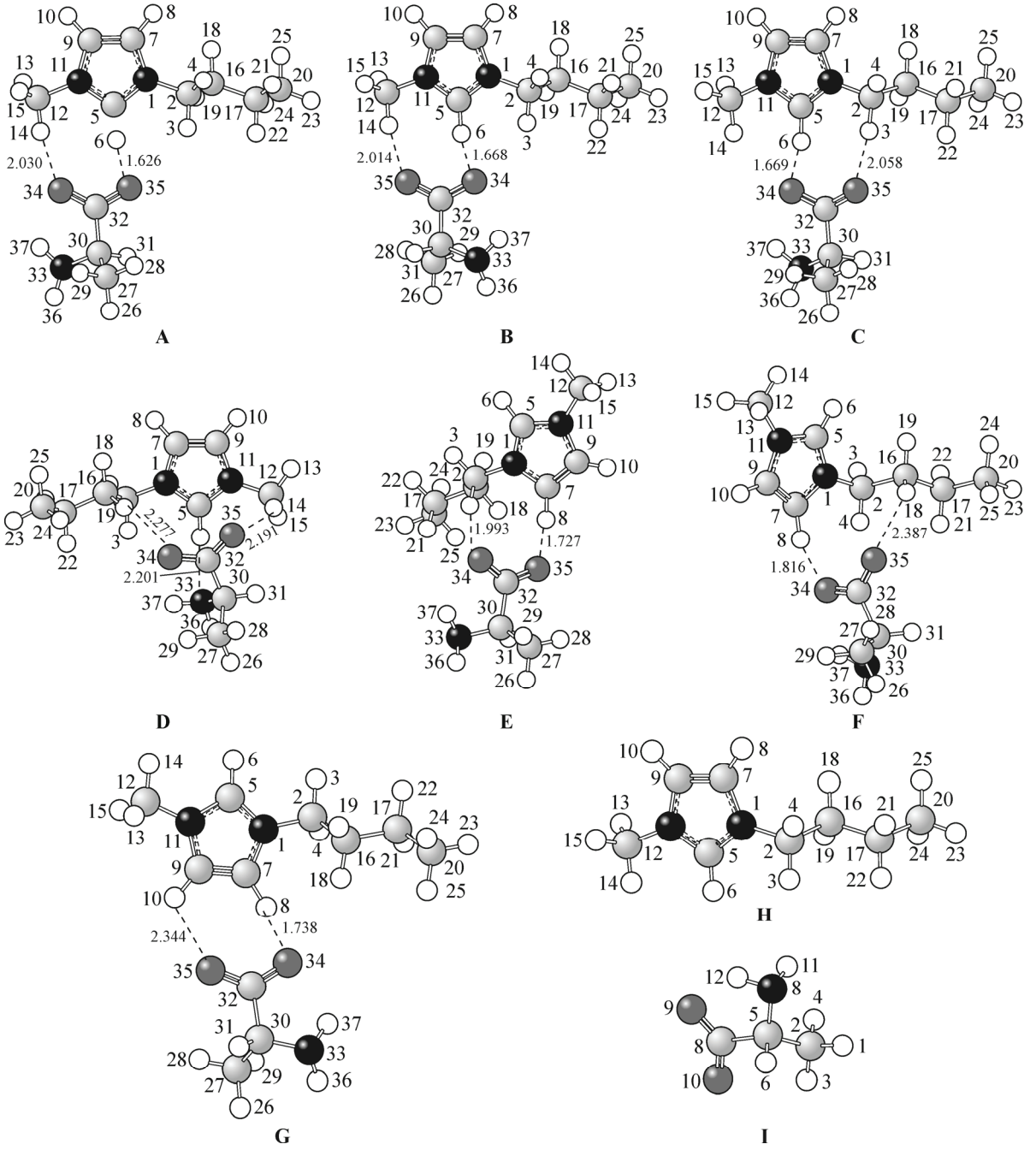

Fig. 1. Optimized structures of the [BMIM][Ala] ionic liquid at the B3PW91/6-311+G(*d*,*p*) level.
All distances are in Angstroms

was shown as **A** in Fig. 1, and two hydrogen bonds between the oxygen atoms of the anion and the hydrogen atoms in methyl and the imidazolium ring of the cation were formed. The lengths of O34—H14 and O35—H6 were 2.030 Å and 1.626 Å respectively, being less than the van der Waals H---O distance (2.72 Å) [37], and obviously, their formation improved the stability of the ion pairs. The structure of the second conformer **B**, which was 2.2 kJ·mol^{-1} less stable than **A**, was very similar to that of **A**. The difference between these two conformers was the hydrogen bonds. In the configuration **B**, the O35—H14 and O34—H6 hydrogen bonds were the main interaction, which were 2.014 Å and 1.668 Å respectively. As shown in Fig. 1, The third conformer **C**, which was 2.6 kJ·mol^{-1} less stable than **A**, was as alike as the aforementioned two structures as a whole.

Table 1

ZPE corrected Relative energies E_r, $kJ \cdot mol^{-1}$, *BSSE and ZPE corrected interaction energies between the anion and the cation* $\Delta E_{BSSE+ZPE}$, $kJ \cdot mol^{-1}$, *and the single point energy change or deformation energies* ΔE_{sp}, $kJ \cdot mol^{-1}$ *of the anion and the cation during the formation of* [BMIM][Ala]

Configuration	E_r	BSSE energy	$\Delta E_{BSSE+ZPE}$	$\Delta E_{sp}/([BMIM]^+)$	$\Delta E_{sp}/([Ala]^-)$
A	0	3.0	385.2	8.8	7.2
B	2.2	3.1	382.9	7.1	7.7
C	2.6	3.3	382.2	7.3	7.6
D	33.2	4.8	350.2	6.2	17.8
E	38.1	3.8	346.3	5.9	6.1
F	46.5	3.8	337.9	6.7	6.7
G	50.4	2.9	334.9	6.4	5.6

The configuration **D**, as illustrated in Fig. 1, was greatly different to the aforesaid three structures. The hydrogen bond between N33 and H6 also formed (2.201 Å), apart from O34—H19 (2.277 Å) and O35—H14 (2.191 Å). Compared with that of **A**, these hydrogen bonds of the configuration **D** were weak and as a result it was 33.2 $kJ \cdot mol^{-1}$ less stable than the most stable conformer **A**. The other isomers of [BMIM][Ala] IL, such as **E**, **F**, and **G** given in Fig. 1, were 38.1 $kJ \cdot mol^{-1}$, 46.5 $kJ \cdot mol^{-1}$, and 50.4 $kJ \cdot mol^{-1}$ less stable respectively. Because the acidity of C5—H in the imidazolium ring was stronger than other H of the cation unit, the hydrogen bond between the C5—H and oxygen of the anion unit must be stronger than other hydrogen bonds and contributed mostly to the stabilities of these structures of the ion pairs. Therefore, the absence of the type of the hydrogen bond formed between C5—H and the oxygen atom in the isomers **D**, **E**, **F**, and **G** would reduce their stabilities relative to **A**, **B**, and **C**. From the above analysis, it could be concluded that in all configurations the hydrogen bonding interactions were mostly between the O atoms on the anion and H atoms on the cation fragments, which possessed more negative and positive charges. The hydrogen bond strength was opposite to its length, and furthermore, the interaction between the cation and the anion was in accordance with the intensity of the hydrogen bond. In the structures of **A**, **B**, and **C** shown in Fig. 1, the hydrogen bond involved C5—H, the acidity of which was the most strong among all the H atoms in the ion pairs, which were shorter than other hydrogen bonds, and as a result, it can be understood easily that these three structures were much more stable relative to the other conformers. In addition, the interactions between the anion and the cation occurred in those regions that possessed more negative and positive charges, suggesting that the electrostatic attractions contributed to the interaction between the anion and the cation.

Furthermore, comparing isolated $[BMIM]^+$ and the ion pairs, it was easily discovered that the C—H bond of the cation would be elongated if the corresponding H atom participated in the formation of the H bond [38]. For example, the bond lengths of C5—H6 and C12—H14 in the configuration **A** changed from 1.078 Å and 1.089 Å in isolated $[BMIM]^+$ to 1.139 Å and 1.097 Å in [BMIM][Ala] **A**. Obviously, the formation of H bonds weakened the corresponding C—H bonds.

INTERACTION ENERGIES

The interaction energies were also calculated and corrected by ZPE and BSSE at the same level, which confirmed the stability order of these conformers from another point of view. As seen from Table 1, these values were 385.2 $kJ \cdot mol^{-1}$, 382.9 $kJ \cdot mol^{-1}$, 82.2 $kJ \cdot mol^{-1}$, 350.2 $kJ \cdot mol^{-1}$, 346.3 $kJ \cdot mol^{-1}$, 337.9 $kJ \cdot mol^{-1}$, and 334.9 $kJ \cdot mol^{-1}$ respectively, being consistent with the stability evaluated by the relative energies. And obviously, it was indubitable that the larger the interaction energy is, the stronger the interaction between the cation and the anion. From a comparison with the results of the structural optimization and the relative energy calculation, it could be seen that because of

the similarity of the geometries of the configurations **A**, **B**, and **C**, their interaction energies were very close. However, these values of the configurations **D**, **E**, **F**, and **G** were all lower than those of **A**, **B**, and **C**, indicating that the difference in the geometries resulted in an inappropriate position for the formation of the hydrogen bonding interaction. The C5—H6 site on $[BMIM]^+$ was the most favorable for the interaction between the anion and the cation because the acidity of H atoms in C7—H8, C9—H10, methyl, and butyl were all weaker than that of C5—H6, and as a result, the interaction energies of **D**, **E**, **F** and **G** conformers were small relative to that of **A**.

In order to evaluate the deformation of ions from the energy point of view, the single point energy changes (ΔE_{sp}) of the anion and the cation during the formation of [BMIM][Ala] IL were obtained by calculating the differences between the free fragment and its corresponding isolated moiety in the ion pairs (the remaining part of the ion pair was set as a ghost atom) [27, 28]. As seen from Table 1, compared with the free anion or the cation, the single point energies of its corresponding isolated unit in the ion pairs changed to a varying degree, suggesting that both anion and cation were distorted during the formation of the ion pairs. As for the $[BMIM]^+$ cation, in all configurations the maximum ΔE_{sp} value was 8.8 $kJ \cdot mol^{-1}$ for **A**, relatively indicating its most prominent change. However, for the anion, the most distinct change took place in the configuration **D**, as revealed by the largest ΔE_{sp} value (17.8 $kJ \cdot mol^{-1}$). It can be speculated rationally that the reason for the deformation during the formation of the ion pairs was the interactions between the anion and the cation, such as the hydrogen bonding interaction and electrostatic attraction.

NBO ANALYSIS

Based on the optimization of the structures for the ion pairs, the natural population and NBO were also calculated at the same level to analyze the charge distribution and bond properties of the ion pairs. Table 2 listed some of the charge increment and decrement values on the corresponding atoms in going from the isolated ions to the ion pairs. It could be seen from Table 2 that there were net charge transfer from the $[Ala]^-$ anion to the $[BMIM]^+$ cation for all configurations during the combination of the two units, and based on the simplicity, only the charge changes on the atoms involving the H bond were listed. The total amount of charge transfer from the anion to the cation for the configura-

Table 2

NBO charge of [BMIM][Ala]

Atoms	[BMIM][Ala]						
	A	**B**	**C**	**D**	**E**	**F**	**G**
H3	+0.027	+0.029	+0.071	+0.009			
H4					+0.071	+0.043	
H6	+0.063	+0.063	+0.063	+0.043			
H8					+0.063	+0.059	+0.060
H10							+0.027
H14	+0.065	+0.067	+0.027	+0.050			
H18					+0.021	+0.0475	+0.034
H19	+0.005	+0.003	+0.002	+0.062			
N33	+0.018	+0.020	+0.019	0	+0.015	+0.016	+0.014
O34	+0.014	–0.010	–0.012	–0.007	+0.005	–0.012	–0.009
O35	–0.008	+0.008	+0.008	+0.017	0	+0.001	0
Total Δe	0.134	0.124	0.122	0.070	0.112	0.084	0.093

Total Δe means the total amount of charge transfer from the anion to the cation, ″–″ means a negative charge increment, ″+″ means a positive charge increment.

Table 3

Electronic donor/acceptor of NBO and the corresponding stable energy of [BMIM][Ala]

Configuration	Donor NBO(i)	Acceptor NBO(j)	$E^{(2)}$, kJ·mol^{-1}	Configuration	Donor NBO(i)	Acceptor NBO(j)	$E^{(2)}$, kJ·mol^{-1}
A	LP(O35)	BD*(1)C5—H6	165.7	**D**	LP(N33)	BD*(1)C5—H6	32.8
	LP(O34)	BD*(1)C12—H14	33.1		LP(O34)	BD*(1)C16—H19	9.9
	BD(1)C32—O35	BD*(1)C5—H6	4.9		LP(O35)	BD*(1)C12—H14	4.9
B	LP(O34)	BD*(1)C5—H6	139.3		BD(C32—O35)	BD*(2)N1—C5	4.7
	LP(O35)	BD*(1)C12—H14	34.7	**E**	LP(O35)	BD*(1)C7—H8	116.5
	BD(C32—O34)	BD*(1)C5—H6	4.7		LP(O34)	BD*(1)C2—H4	32. 2
C	LP(O34)	BD*(1)C5—H6	137.9	**F**	LP(O34)	BD*(1)C7—H8	79.5
	LP(O35)	BD*(1)C2—H3	30.0		LP(O35)	BD*(2)C7—C9	3.9
	BD(C32—O34)	BD*(1)C5—H6	4.4	**G**	LP(O34)	BD*(1)C7—H8	107.1

tion **A** was the maximum, being in agreement with its maximum interaction energy. However, for some configurations, the relationship did not hold true. In addition, on the H, O, and N atoms, which formed H bonds with each other between the anion and cation fragments, the charge accumulations were relatively prominent. For example for the configuration **A**, both H6 and H14 formed H bonds with O35 and O34 respectively, therefore, during the formation of the ion pairs, the evident charge transfer occurred on H6 and H14. The rest of the configurations also exhibit this feature. Based on the above analysis, it could be concluded that during the combination of the $[Ala]^-$ anion and the $[BMIM]^+$ cation, the charge redistribution mainly took place on the corresponding atoms involving H bonds. Rationally, the charge transfer and redistribution also contributed to the stability of the ion pairs.

The second order interaction energies ($E^{(2)}$) of IL can be used to investigate the interaction between the cation and the anion, electron donor orbitals, electron acceptor orbitals, which indicates the intensity of the interaction between the electron donor orbitals and the electron acceptor orbitals [39]. The higher the value of $E^{(2)}$ is, the more the electron tends to transfer from donor orbitals to acceptor orbitals. It can be obtained from the following equation: $E^{(2)} = q_i \times F_{(i,j)}^2/(\varepsilon_I - \varepsilon_j)$, where q_i is the donor orbital occupancy, ε_i and ε_j are the diagonal elements, and $F_{(i,j)}$ is the off-diagonal NBO Fock matrix element. The $E^{(2)}$ values were also computed and listed in Table 3, in which LP and BD* denote the lone pairs and antibonding orbitals respectively. As seen from Table 3, for the most stable structure **A**, the second order interaction energies of LPs of O35 and BD* of C5—H6 were maximal (165.7 kJ·mol^{-1}), contributing mostly to the stability of the ion pairs, and indicating that the hydrogen bond between O35 and C5—H6 was stronger than other hydrogen bonds. Therefore, the interaction of the cation and the anion was dominated by a hydrogen bond formed by LPs of O35 and C5—H6 antibond. However, the interaction between LPs of O34 and the antibond of C12—H14 also promoted its stability. As for the structure of **B**, the dominant interaction between the $[BMIM]^+$ and $[Ala]^-$ fragments presented to be the interaction of LPs of O34 and BD* of C5—H6, whose $E^{(2)}$ amounted to 139.3 kJ·mol^{-1}. The interaction due to O35 and C12—H14, which amounted to 34.7 kJ·mol^{-1}, was relatively small. In regard to the configuration **C**, the second order interaction energy resulted from the hydrogen bonds between O34 and C5—H6 was also maximum, predicating that it was the strongest interaction. From the above analysis of the configurations **A**, **B**, and **C**, it can be seen that there were some similarities, i.e. the dominant interactions all involved C5—H6 in the imidazole plane, whose acidity was the strongest among all of the H atoms.

As regards the configuration **D**, the primary donor NBO was LPs of N33 in the anion unit, while the acceptor NBO was the antibond of C5—H6 in the cation unit, which was different from the other conformers. Additionally, the $E^{(2)}$ value was also smaller than those of the other systems. The $E^{(2)}$ values for the configurations **E**, **F**, and **G**, also indicated that the primary interactions resulted from LPs of O34 or O35 and the C7—H8 antibond, as seen from Table 3. Comparing $E^{(2)}$ with the interaction

energies it can be concluded that the large $E^{(2)}$ values for the configurations **A**, **B**, and **C** may be one of the leading causes of their large interaction energies.

CONCLUSIONS

Based on the calculation of the electron structure for IL of the 1-butyl-3-methylimidazolium cation and the alanine anion, i.e. [BMIM][Ala], the configurations in the gas phase with different stabilities were obtained. The BSSE and ZPE corrected interaction energies between the anion and the cation were in turn 385.2 kJ·mol^{-1}, 382.9 kJ·mol^{-1}, 382.2 kJ·mol^{-1}, 350.2 kJ·mol^{-1}, 346.3 kJ·mol^{-1}, 337.9 kJ·mol^{-1}, and 334.9 kJ·mol^{-1}, and the larger the value is, the stronger the interaction. The hydrogen bonding interaction and electrostatic attraction were the main modes of the interaction between the anion and the cation, and they both contributed to the stabilities of the system. Configurations **A**, **B**, and **C** were more stable structures, and their interaction energies were close to each other. During the combination of the cation and the anion, geometry changes, charge redistribution, and hydrogen bonding interaction enhanced the stability. In the most stable structure, the hydrogen bond formed between LPs of O35 and the antibond of C5—H6 was the strongest and contributed mostly to the stability of the configuration, the second order interaction energy of which also confirmed its stability from another point of view. The interaction between the anion and the cation included the electrostatic power and the hydrogen bond, and delocalization resulting from the transfer of LPs of the O atom in the anion to the antibond contributed mostly to the stability.

REFERENCES

1. *Liu S., Xie C., Yu S., Liu F.* // Catal. Commun. – 2009. – **10**, N 6. – P. 986.
2. *Fang S., Yang L., Wang J., Li M., Tachibana K., Kamijima K.* // Electrochim. Acta. – 2009. – **54**, N 17. – P. 4269.
3. *Parvulescu V.I., Hardacre C.* // Chem. Rev. – 2007. – **107**, N 6. – P. 2615.
4. *Plechkova N.V., Seddon K.R.* // Chem. Soc. Rev. – 2008. – **37**, N 1. – P. 123.
5. *Rogers R.D., Seddon K.R.* // Science. – 2003. – **302**, N 5646. – P. 792.
6. *Ranu B.C., Jana R., Sowmiah S.* // J. Org. Chem. – 2007. – **72**, N 8. – P. 3152.
7. *Gong K., Wang H.L., Fang D., Liu Z.L.* // Catal. Commun. – 2008. – **9**, N 5. – P. 650.
8. *Fukumoto K., Yoshizawa M., Ohno H.* // J. Amer. Chem. Soc. – 2005. – **127**, N 8. – P. 2398.
9. *Ohno H., Fukumoto K.* // Acc. Chem. Res. – 2007. – **40**, N 11. – P. 1122.
10. *Fukumoto K., Ohno H.* // Chem. Commun. – 2006. – **29**, 3081.
11. *Tao G.H., He L., Sun N., Kou Y.* // Chem. Commun. – 2005. – **28**, 3562.
12. *Tao G.H., He L., Liu W., Xu L., Xiong W., Wang T., Kou Y.* // Green Chem. – 2006. – **8**, N 7. – P. 639.
13. *Plaquevent J.C., Levillain J., Guillen F., Malhiac C., Gaumont A.C.* // Chem. Rev. – 2008. – **108**, N 12. – P. 5035.
14. *Chen X., Li X., Hu A., Wang F.* // Tetrahedron: Asymmetry. – 2008. – **19**, N 1. – P. 1.
15. *Siyutkin D.E., Kucherenko A.S., Struchkova M.I., Zlotin S.G.* // Tetrahedron Lett. – 2008. – **49**, N 7. – P. 1212.
16. *Zhou L., Wang L.* // Chem. Lett. – 2007. – **36**, N 5. – P. 628.
17. *Brégeon D., Levillain J., Guillen F., Plaquevent J.C., Gaumont A.C.* // Amino Acids. – 2008. – **35**, N 1. – P. 175.
18. *Jiang Y.Y., Wang G.N., Zhou Z., Wu Y.T., Geng J., Zhang Z.B.* // Chem. Commun. – 2008. – **4**. – P. 505.
19. *Wu F., Dou X.Y., He L.N., Miao C.X.* // Lett. Org. Chem. – 2010. – **7**, N 1. – P. 73.
20. *Mou Z.X., Li P., Wang W., Shi J., Song R.* // J. Phys. Chem. B. – 2008. – **112**, N 16. – P. 5088.
21. *Rong H., Li W., Chen Z.Y., Wu X.M.* // J. Phys. Chem. B. – 2008. – **112**, N 5. – P. 1451.
22. *Gao H.Y., Zhang Y., Wang H.J., Liu J.H., Chen J.M.* // J. Phys. Chem. A. – 2010. – **114**, N 37. – P. 10243.
23. *Chiappe C., Signori F., Valentini G., Marchetti L., Pomelli C.S., Bellina F.* // J. Phys. Chem. B. – 2010. – **114**, N 15. – P. 5082.
24. *Zhang L., Li H.R., Wang Y., Hu X.B.* // J. Phys. Chem. B. – 2007. – **111**, N 37. – P. 11016.
25. *Gutowski K.E., Holbrey J.D., Rogers R.D., Dixon D.A.* // J. Phys. Chem. B. – 2005. – **109**, N 49. – P. 23196.
26. *Gutowski K.E., Rogers R.D., Dixon D.A.* // J. Phys. Chem. B. – 2007. – **111**, N 18. – P. 4788.
27. *Zhang Y., Chen X.Y., Wang H.J., Diao K.S., Chen J.M.* // J. Mol. Struct. THEOCHEM. – 2010. – **952**, N 1. – P. 16.
28. *Wu Y., Zhang T.* // J. Phys. Chem. A. – 2009. – **113**, N 46. – P. 12995.

29. *Becke A.D.* // J. Chem. Phys. – 1993. – **98**, N 7. – P. 5648.
30. *Perdew J.P., Burke K., Wang Y.* // Phys. Rev. B. – 1996. – **54**, N 23. – P. 16533.
31. *Milet A., Korona T., Moszynski R., Kochanski E.* // J. Chem. Phys. – 1999. – **111**, N 17. – P. 7727.
32. *Reed A.E., Weinstock R.B., Weinhold F.* // J. Chem. Phys. – 1985. – **83**, N 2. – P. 735.
33. *Reed A.E., Curtiss L.A., Weinhold F.* // Chem. Rev. – 1988. – **88**, N 6. – P. 899.
34. *van Duijineveldt F.B., van Duijineveldt-van de Rijdt J.G.C.M., van Lenthe J.H.* // Chem. Rev. – 1994. – **94**. – P. 1873.
35. *Boys S.F., Bernardi F.* // Mol. Phys. – 1970. – **19**, N 5. – P. 553.
36. *Frisch M.J., Trucks G.W., Schlegel H.B. et al.* Gaussian 03, Revision C.02, Gaussian, Inc., Wallingford CT, 2004.
37. *Bondi A., van der Waals* // J. Phys. Chem. – 1964. – **68**, N 3. – P. 441.
38. *Ren X.H., Wang H.J.* // J. Solution Chem. – 2009. – **38**, N 3. – P. 303.
39. *Miehlich B., Savin A., Stoll H., Preuss H.* // Chem. Phys. Lett. – 1989. – **157**, N 1/2. – P. 200.